

Marquette University
e-Publications@Marquette

Chemistry Faculty Research and Publications

Chemistry, Department of

1-1-2016

Hydrogen-atom Attack on Phenol and Toluene is *ortho*-directed

Olha Krechkivska
University of New South Wales

Callan M. Wilcox
University of New South Wales

Tyler P. Troy
University of Sydney

Klaas Nauta
University of New South Wales

Bun Chan
University of Sydney

See next page for additional authors

Accepted version. *Physical Chemistry Chemical Physics*, Vol. 18, No. 12 (2016): 8625-8636. DOI. ©
2016 Royal Society of Chemistry. Used with permission.

Authors

Olha Krechkivska, Callan M. Wilcox, Tyler P. Troy, Klaas Nauta, Bun Chan, Rebecca Jacob, Scott A. Reid, Leo Radom, Timothy W. Schmidt, and Scott H. Kable

Marquette University

e-Publications@Marquette

Faculty Research and Publications/Department of Chemistry

This paper is NOT THE PUBLISHED VERSION; but the author's final, peer-reviewed manuscript. The published version may be accessed by following the link in the citation below.

Physical Chemistry Chemical Physics, Vol. 18, No. 12 (2016): 8625-8636. [DOI](#). This article is © [Royal Society of Chemistry] and permission has been granted for this version to appear in [e-Publications@Marquette](#). [Royal Society of Chemistry] does not grant permission for this article to be further copied/distributed or hosted elsewhere without the express permission from [Royal Society of Chemistry].

Hydrogen-atom attack on phenol and toluene is ortho-directed

Olha Krechkivska

School of Chemistry, University of New South Wales, Kensington, NSW 2052, Australia

Callan M. Wilcox

School of Chemistry, University of New South Wales, Kensington, NSW 2052, Australia

Tyler P. Troy

School of Chemistry, University of Sydney, Sydney, NSW 2006, Australia

Klaas Nauta

School of Chemistry, University of New South Wales, Kensington, NSW 2052, Australia

Bun Chan

School of Chemistry, University of Sydney, Sydney, NSW 2006, Australia

Rebecca Jacob

School of Chemistry, University of Sydney, Sydney, NSW 2006, Australia

Scott A. Reid

Department of Chemistry, Marquette University, Milwaukee, WI

Leo Radom

School of Chemistry, University of Sydney, Sydney, NSW 2006, Australia

Timothy W. Schmidt

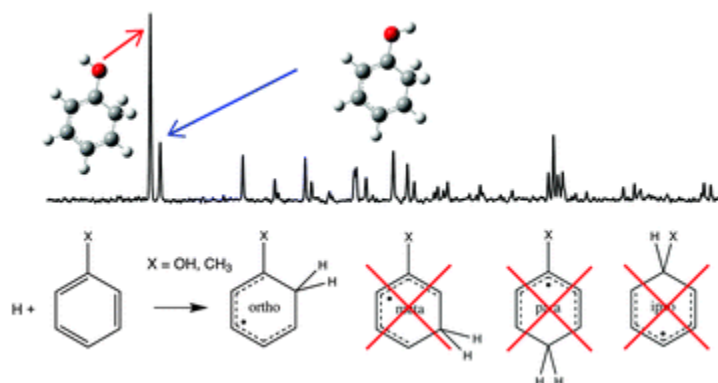
School of Chemistry, University of New South Wales, Kensington, NSW 2052, Australia

Scott H. Kable

School of Chemistry, University of New South Wales, Kensington, NSW 2052, Australia

Abstract

The reaction of H + phenol and H/D + toluene has been studied in a supersonic expansion after electric discharge. The (1 + 1') resonance-enhanced multiphoton ionization (REMPI) spectra of the reaction products, at $m/z = \text{parent} + 1$, or $\text{parent} + 2$ amu, were measured by scanning the first (resonance) laser. The resulting spectra are highly structured. Ionization energies were measured by scanning the second (ionization) laser, while the first laser was tuned to a specific transition. Theoretical calculations, benchmarked to the well-studied H + benzene \rightarrow cyclohexadienyl radical reaction, were performed. The spectrum arising from the reaction of H + phenol is attributed solely to the *ortho*-hydroxy-cyclohexadienyl radical, which was found in two conformers (*syn* and *anti*). Similarly, the reaction of H/D + toluene formed solely the *ortho* isomer. The preference for the *ortho* isomer at 100–200 K in the molecular beam is attributed to kinetic, not thermodynamic effects, caused by an entrance channel barrier that is ~ 5 kJ mol⁻¹ lower for *ortho* than for other isomers. Based on these results, we predict that the reaction of H + phenol and H + toluene should still favour the *ortho* isomer under elevated temperature conditions in the early stages of combustion (200–400 °C).



Introduction

Addition, loss, and transfer of hydrogen atoms constitute some of the most fundamental processes in chemistry. Loss of a hydrogen atom is the first chemical step in most combustion processes.¹ OH radical abstraction of H starts the atmospheric oxidative process for many airborne organic compounds, and further abstraction of H from free radicals by O₂ continues the pathway.² Intramolecular H-atom transfer promotes isomerization, for example, gas-phase keto–enol tautomerization.³ Hydrogenation and dehydrogenation of polycyclic aromatic hydrocarbons (PAHs) are also hypothesized to occur in the interstellar medium.^{4–6} Indeed, throughout chemistry, the energetic and kinetic battle between molecules, radicals and ions in competition for H atoms is prevalent throughout all complex reaction mechanisms.

Aromatic molecules constitute a large fraction of many liquid fuels, including automotive petroleum/gasoline. The Australian standard allows automotive fuel to comprise up to 45% aromatics by weight.⁷ The addition of H₂ to such aromatic fuel mixtures has long been known to result in a much lower production of soot, which is largely comprised of PAHs.⁸ The effectiveness of H₂ in reducing soot formation has been attributed to sequential addition of H atoms to the aromatic core, until the ring is entirely saturated. For example, benzene is converted to cyclohexane, toluene to methylcyclohexane.⁹

Despite extensive modelling of H-addition to aromatic compounds, the intermediate H-adducted radicals have rarely been detected. The cyclohexadienyl radical itself (H + benzene) is well characterized.^{10–13} Additionally, several reports characterizing the hydronaphthyl radical (H + naphthalene) have been reported recently.^{14–18} However, the spectroscopy, structure, energetics and kinetics of H-addition to other common aromatics, such as toluene and phenol, are largely unreported.

In this paper, we report the spectroscopic characterization of radicals formed from H-addition to two singly-substituted aromatic molecules – phenol and toluene. Toluene and phenol are prototypical functionalized benzene compounds that also find general application. Toluene is a common fuel additive. H-atom attack leads to one of four isomeric methyl-cyclohexadienyl (methyl-CHD) radicals (Fig. 1), and is an important combustion reaction. H-addition to phenol leads to the hydroxy-cyclohexadienyl (hydroxy-CHD) radical. The ipso isomer of this radical (Fig. 1) is the same species that is formed from OH attack on benzene, which is the postulated first reaction in the oxidation of aromatic species in the atmosphere.¹⁹

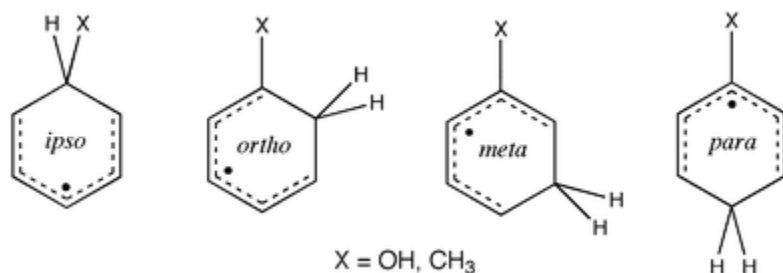


Fig. 1 Four structural isomers of a singly-substituted cyclohexadienyl radical.

Previous work on CHD, hydroxy-CHD and methyl-CHD

The D₁–D₀ energies and ionization energies (IEs) of hydroxy- and methyl-CHD are key experimental observables in the present work. Comparison with the results of quantum chemistry computations allows us to decide which isomers are observed. Cyclohexadienyl radical is used to benchmark our theoretical methods because both the D₁–D₀ transition^{10–12} and IE are well-known,¹³ and there have been two recent computational studies with which to compare our methods.^{13,20}

The electronic absorption spectrum of the CHD radical was first reported in 1963 in a frozen (77 K) matrix of 3-methylpentane, revealing two maxima near 310 nm.²¹ Several measurements have been made subsequently,^{22,23} concluding that this transition corresponds to excitation of the second excited electronic state. The D₁(²A₂)–D₀(²B₁) electronic band system of CHD was found to lie in the visible region of the spectrum, near 550 nm.¹⁰ High-resolution laser-induced fluorescence (LIF) spectra in the gas

phase identified the electronic origin at $18\,207\text{ cm}^{-1}$.^{10–12} The IE of CHD has been reported recently to be $6.820(1)\text{ eV}$.¹³

Experimental^{24–26} and theoretical^{27–30} investigations of hydroxy-CHD have mostly approached this species from the benzene + OH side because of the atmospheric relevance. A consequence, however, is that the ipso form of the radical has been almost solely considered; the ortho, meta and para forms have received much less attention. Hydroxy-CHD has been detected in the gas phase by UV absorption spectroscopy via the D_2 – D_0 transition, near 300 nm .^{26,30} The UV spectrum is broad, like CHD.³⁰ Neither the D_1 – D_0 spectrum, nor the IE, has been reported for any isomer.

The methyl-CHD radical has received relatively little attention. Uc et al. have calculated the relative stability, ΔH_r (298 K), of all four methyl-CHD isomers relative to toluene + H.³¹ Tokmakov and Lin calculated the reaction profile for $\text{H} + \text{toluene} \rightarrow \text{ipso-methyl-CHD}$ and thence to benzene + CH_3 .³² They also calculated the barrier to the [1,2]-H shift between ipso and ortho isomers to be vastly in excess of the C–H bond energy. To our knowledge, the electronic spectroscopy of methyl-CHD has not been reported.

Experimental and computational methods

Experimental

Experiments were carried out in a resonance-enhanced multiphoton ionization (REMPI) chamber equipped with a time-of-flight (ToF) mass spectrometer that has been described previously.³³ The vapor of phenol or toluene (Aldrich, used as supplied) was co-expanded with $\text{H}_2\text{O}/\text{D}_2\text{O}$ in a free jet expansion using Ar carrier gas at a seed ratio of ~ 0.1 – 1% organic, $\sim 1\%$ water at a total pressure of 6–7 bar. The gas mixture entered the vacuum via a pulsed nozzle equipped with a pair of electrodes. During the gas pulse, a short ($80\ \mu\text{s}$) high-voltage pulse (1.6 kV with 25 k Ω ballast resistor) sparked an electric discharge. During the discharge, metastable Ar atoms collide with $\text{H}_2\text{O}/\text{D}_2\text{O}$ molecules, fragmenting them to $\text{H} + \text{OH}$ ($\text{D} + \text{OD}$) with high efficiency.³⁴ H/D atoms in turn collide with the aromatic species. In the high-pressure region of the expansion, there are sufficient three-body collisions to stabilize the H-adducted radicals.

The expansion is passed through a skimmer ($\varphi = 2\text{ mm}$) forming a collimated molecular beam in the ionization chamber. The beam was intersected with two tunable ns-pulsed laser beams, counter-propagating and coincident in time. The first beam (Nd:YAG-pumped dye laser) excited the D_1 – D_0 transition in the H-adducted radical, which was near 550 nm in each case (C540A dye). A second Nd:YAG-pumped dye laser, tuned near 300 nm (R610 dye and a BBO doubling crystal), served to ionize the excited radical.

The closed-shell cation formed after REMPI was accelerated in a ToF mass spectrometer and detected via a multichannel plate detector. The signal on the m/z (parent + 1 or parent + 2) mass was monitored as a function of either laser wavelength or delay time between lasers. Scanning the first laser, with the second laser well above the ionization threshold, provided a REMPI spectrum of the D_1 – D_0 transition of the radical. Scanning the second (ionization) laser while holding the first laser on a resonance provided a photoionization efficiency (PIE) spectrum and hence the ionization energy.

Hole-burning experiments were performed to distinguish different isomers. In these experiments, the two lasers used above were tuned to a peak in the REMPI spectrum. A third laser (Nd:YAG-pumped dye laser) intersected the molecular beam about 100 ns before the REMPI lasers. This laser was scanned across the same wavelength range as the D_1 - D_0 spectrum and was used to “bleach” the population of whichever radical was in resonance with that laser. If the isomer was the same as being probed by REMPI, then the bleach results in a smaller REMPI signal. If the bleach laser depletes a different isomer, then the REMPI signal is unaffected. In this way, an isomer-specific hole-burning spectrum (depletion of REMPI signal) is measured as a function of bleach wavelength.

Theoretical

Standard ab initio and density functional theory (DFT) calculations were carried out using the Gaussian 09³⁵ and MOLPRO 2010³⁶ programs. Lower-level calculations were carried out using the (TD)-B3-LYP DFT procedure and appropriate basis sets. Higher-level calculations were carried out with composite methods that aim to approximate CCSD(T) with an infinite basis set, either by additivity and empirical corrections, or via extrapolation. The former category includes G3X(MP2)-RAD³⁷ and G4(MP2)-6X,³⁸ while the latter includes W1X-1³⁹ and W1X-2,³⁹ with W1X-1 being slightly more accurate.³⁹

Geometries for the G3X(MP2)-RAD calculations were optimized at the B3-LYP/6-31G(2df,p) level. The resulting single-point energies were corrected (where indicated) with zero-point energies (zpe's) and thermal corrections, derived from scaled (0.9854) B3-LYP/6-31G(2df,p) harmonic vibrational frequencies, to provide enthalpies at 0 K and 298 K. For the G4(MP2)-6X procedure, geometries were optimized at the BMK/6-31+G(2df,p) level,⁴⁰ and the energies corrected to enthalpies at 0 K and 298 K using zpe and thermal corrections, derived from scaled (0.9770 and 0.9627, respectively) BMK/6-31+G(2df,p) harmonic vibrational frequencies.⁴¹ The geometries for W1X-1 and W1X-2 were obtained using B3-LYP/cc-pVTZ+d. Scaled (by 0.985) B3-LYP/cc-pVTZ+d harmonic vibrational frequencies were used to obtain zpe's and thermal corrections, which were incorporated as required to give enthalpies at 0 K and 298 K.³⁹

Results

Theoretical benchmarking study

Computational chemistry is an important ingredient in the assignment of the carriers of the m/z 95 (H + phenol) and m/z 93 (H + toluene) spectra. Therefore we performed a series of benchmarking calculations on the cyclohexadienyl (CHD) radical.

Several groups have calculated ionization and bond energies of the CHD radical.^{20,42,43} The most recent, and highest level calculations, were performed by Botschwina and co-workers, who reported various ionization and bond-breaking properties of CHD using explicitly correlated coupled cluster theory at the (R)CCSD(T)-F12 level.²⁰ The calculated ionization energy was 6.803(5) eV, which compares very favourably with the new experimental result, 6.8201(5) eV,¹³ although the computational error seems to be slightly underestimated. We use these computational results and a variety of experimental results for benchmarking our computational methods.

[Table 1](#) shows calculated values of the IE of CHD, the proton affinity of benzene, and the strength of the C–H bond in both C_6H_7 and $C_6H_7^+$, for several theoretical procedures and basis sets. DFT is computationally efficient, and has been shown to produce good nuclear geometries and vibrational frequencies.²⁰ However, it performs less well in reproducing ionization and bond-breaking energies with an IE that is 300 meV lower than the previous (R)CCSD(T*) calculation and a proton affinity that is 60 kJ mol⁻¹ too high, compared with experiment ([Table 1](#)).^{44–46}

Table 1 Experimental and theoretical results on the cyclohexadienyl radical. All units are kJ mol⁻¹, except for the ionization energy, which is reported in eV

Level of theory	Ionization energy (eV)	C_6H_6 proton affinity	$C_6H_7 \rightarrow C_6H_6 + H$	$C_6H_7^+ \rightarrow C_6H_6^+ + H$
a Ref. 20 . b 0 K, ref. 13 . c 298 K. This is the average of two recommended values by NIST, (ref. 44) from original ref. 45 and 46 . d 298 K. This value was determined from the thermodynamic cycle involving the experimental IEs of H-atom and benzene (ref. 44) and the experimental proton affinity of benzene in the table.				
B3-LYP/6-31G(2df,p)	6.45	810	119	352
B3-LYP/6-311++G(3df,3pd)	6.69	788	114	351
G3X(MP2)-RAD	6.86	765	110	355
G4(MP2)-6X vibrationless	6.85	766	107	353
G4(MP2)-6X (zpe corrected, 0 K)	6.90	740	85	322
G4(MP2)-6X (zpe corrected, 298 K)	6.90	744	90	328
W1X-1 vibrationless	6.79	768	110	356
W1X-1 (zpe corrected, 0 K)	6.84	742	88	323
W1X-1 (zpe corrected, 298 K)	6.84	746	93	330
(R)CCSD(T*) vibrationless ^a	6.75	—	107	—
(R)CCSD(T*) (zpe corr., 0 K) ^a	6.803(5)	—	85.7	—
(R)CCSD(T*) (zpe-corr., 298 K) ^a	—	—	89.2	—
Experiment	6.8201	748.4	—	328.2

Higher-level electronic structure calculations were performed at the optimized B3-LYP/6-31G(2df) geometry. The three ab initio methods, G3X(MP2)-RAD, G4(MP2)-6X and W1X-1, and to a lesser extent, B3-LYP with a larger basis set, all perform much better and we benchmark them against (R)CCSD(T*)²⁰ and experiment.¹³ For neutral C_6H_7 , the vibrationless (pure electronic) energies are all within 100 meV

for the IE, and within 3 kJ mol⁻¹ for the C–H bond energy of the previous (R)CCSD(T*) results.²⁰ When corrected for zpe, the IE calculated using W1X-1 is very close to the experimental measurement. Indeed the W1X-1 and (R)CCSD(T*) calculations bracket the experimental IE, with the deviations in each case being only 20 meV. When a thermal correction is applied to the 0 K values, the W1X-1 bond energy and proton affinity at 298 K are within 4 kJ mol⁻¹ of the experimental (298 K) values.

G3X(MP2)-RAD and G4(MP2)-6X theory are slightly less accurate than W1X-1 and (R)CCSD(T) for the four experimental observables in [Table 1](#), but are computationally more efficient. Specifically, the zpe-corrected ionization energy is over-estimated by 80 meV and we use this as an empirical correction factor for G4(MP2)-6X in estimating IEs for the larger radicals below.

H-addition to phenol: hydroxy-cyclohexadienyl radical (hydroxy-CHD)

[Fig. 2a](#) shows the (1 + 1') REMPI spectrum of the species at m/z 95 from a discharge of phenol and water in argon that has been expanded in a molecular beam. The two strongest peaks, near 18 200 cm⁻¹, are separated by only 18 cm⁻¹, in the region that we associate with the D₁ ← D₀ electronic origin transition.

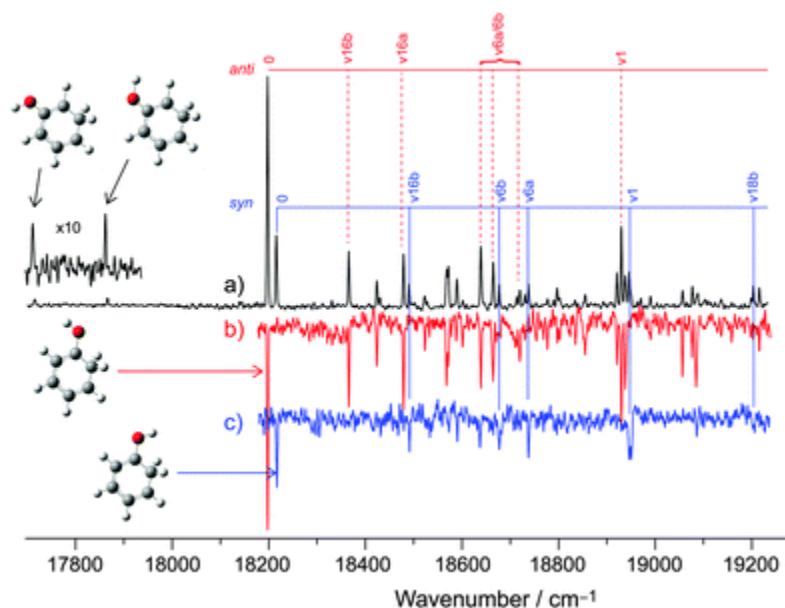


Fig. 2 (a) REMPI spectrum of m/z 95 species from H-addition to phenol. The carrier of the spectrum is assigned to be the syn and anti conformers of the ortho-hydroxycyclohexadienyl radical, as shown by comparison with the hole-burning spectra. (b and c) Vibrational assignments of the most intense structure are shown above the REMPI spectrum, based on ab initio calculations of the D₁ state of each conformer. Small features to the red of the main spectrum are tentatively assigned to the meta-hydroxy-CHD radical (see text).

Photoionization efficiency (PIE) curves were recorded following excitation of these two strongest peaks, as shown in [Fig. 3](#). The IEs shown in the figure were recorded with an extraction field of 206 V, which lowers the true IE slightly. We have previously measured the effect of the electric field on the IE of methyl-CHD and found that the extrapolated zero-field IE was 8 ± 1 meV higher than measured under these operating conditions.¹³ While different molecules will be affected differently by an

external field, the orbitals from which the electron is ejected in methyl-CHD and hydroxy-CHD are similar. Therefore the correction from observed to zero-field IE should also be very similar for both molecules, and we have used the same correction factor for both. These corrected values are shown in [Table 2](#). The ionization thresholds for the two isomers are very close, differing by only 10.2 meV (82 cm^{-1}). However, this is considerably in excess of our experimental uncertainty, which we estimate at $<1\text{ meV}$ (8 cm^{-1}), which reinforces the finding that there are two isomers present in the spectrum.

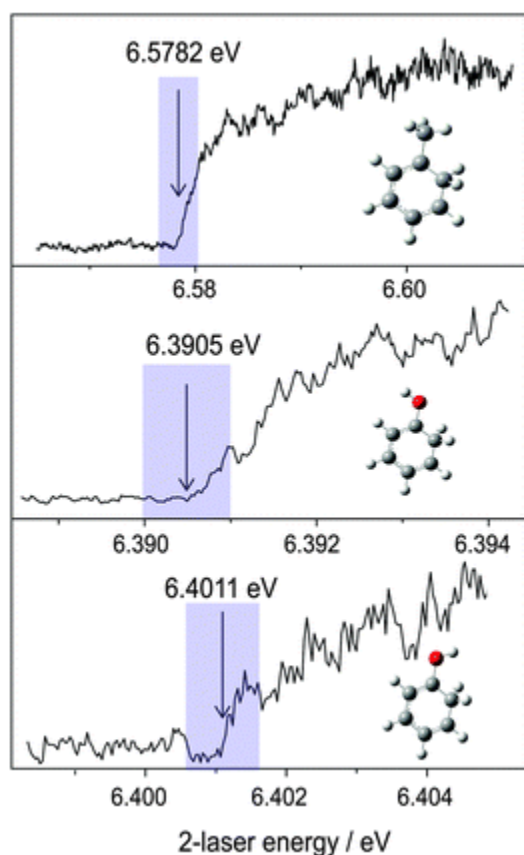


Fig. 3 Photoionization efficiency curves for the three molecules studied in this work. The ionization energies indicated in the figure are for the molecules in a 206 V electric field, which lowers the IE by 8 meV. Corrected IEs are reported in [Tables 1–3](#). Shaded regions represent an experimental uncertainty of 0.5 meV for methyl-CHD and 1 meV for hydroxy-CHD.

Table 2 Computational results for various thermochemical properties of the four isomers of hydroxycyclohexadienyl radical. Results are presented for the G4(MP2)-6X level of theory; results for other levels of theory are reported in ESI. All values in kJ mol^{-1} , except for the IE, in eV

Property of hydroxy-CHD	ortho	meta	para	ipso
Geometries optimized at B3-LYP/6-31G(2df,p).				
Relative energy	0.0	13.5	13.1	32.0
Relative energy of cation	14.4	73.3	0.0	123.7
C–H bond dissociation energy, vibrationless	119	106	106	87
C–H BDE, zpe corrected, 0 K	97	85	85	66
Ionization energy, vibrationless (eV)	6.39	6.86	6.11	7.19
Ionization energy, zpe corrected, 0 K (eV)	6.47	6.94	6.19	7.27
Ionization energy, empirically corrected, 0 K (eV)	6.39	6.86	6.11	7.19
Ionization energy, corrected experimental (eV)	6.3989 and 6.4091 (±0.0010)			

Two hole-burning spectra were measured, shown reflected below the REMPI spectrum in [Fig. 2](#). In this experiment, the REMPI lasers were tuned to the frequency of one of the major peaks at 18 200 (spectrum b) or 18 218 cm^{-1} (spectrum c). The bleach laser, 100 ns earlier in time, was scanned through the same region. The hole-burning spectra show clearly that the two major peaks near 18 200 cm^{-1} belong to different isomers. Additionally, the two hole-burning spectra identify every major peak in the spectrum with one or the other isomer. Therefore we conclude that the REMPI spectrum in the region shown in [Fig. 2a](#) comprises only 2 isomers.

Finally, the ionization laser was scanned in time across the laser responsible for $D_1 \leftarrow D_0$ excitation. This temporal scan, shown in ESI,† was fit to a convolution of an 8 ns Gaussian function (the instrument function) and a decaying exponential function to provide an estimated lifetime of the D_1 state of 4 ± 1 ns.

There are four structural isomers of the hydroxy-CHD radical, formed from H-addition to the benzene ring in the ortho, meta, para and ipso positions with respect to the hydroxyl group ([Fig. 1](#)). We turn to theory to distinguish which of the four isomers are the carriers of the observed spectrum.

[Table 2](#) shows selected computational results for the four isomers of hydroxy-CHD at the G4(MP2)-6X level of theory. The most directly comparable quantity for distinguishing between the isomers is the IE. Based on the benchmark studies against CHD, we expect the calculated G4(MP2)-6X value to overestimate the experimental IE by about 80 meV. [Table 2](#) shows the predicted IEs, using our empirical correction factor for all four isomers. Experimentally, two IEs were measured: 6.399(1) and 6.409(1) eV. Only one computational IE lies near these values – the corrected IE of ortho-hydroxy-CHD was calculated to be 6.39 eV. The IE's of all other isomers lie >0.25 V higher or lower than the experimental values and therefore we conclude that para, meta and ipso-hydroxy-CHD are not the carriers of the spectrum.

A potential energy scan of the OH torsional angle, with other coordinates optimized at each OH angle, [Fig. 4](#), shows that there are two conformers of the ortho-hydroxy-CHD radical. The anti isomer lies

about 450 cm^{-1} to lower energy than syn, with a 1750 cm^{-1} barrier (measured from the anti side) between them. The relative energies are sufficiently similar and the interconversion barrier sufficiently high, that both rotamers are likely to be formed in the expansion.

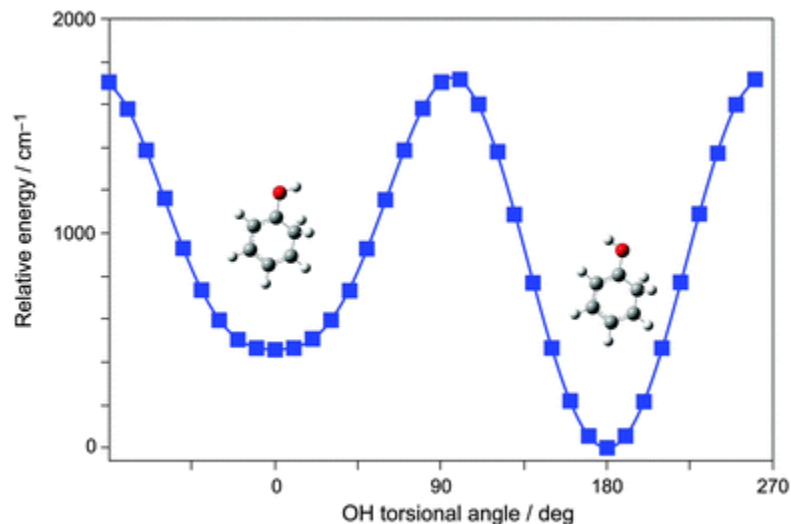


Fig. 4 Potential energy scan of the OH torsional angle in ortho-hydroxy-CHD, computed at the B3-LYP/6-311++g(d,p) level of theory.

To further explore the REMPI spectra, we performed TD-DFT (B3LYP/cc-pvtz) calculations on the D_1 excited states of both syn and anti-ortho-hydroxy-CHD radical. [Table 3](#) shows the calculated vertical transition energy, zero-point energy (zpe) corrected energy and oscillator strength for these species with the same calculations for the CHD radical shown for comparison. In CHD, the experimental D_1 - D_0 transition energy is 2230 cm^{-1} lower than the calculation,^{11,12} the D_1 - D_0 transition energies of both syn and anti isomers of ortho-hydroxy-CHD are over-estimated by a similar amount. The transition in the anti isomer is predicted to be of lower energy than the syn, although the computational difference is greater than the experimental difference. The oscillator strength is calculated to be about twice as strong for the anti conformer compared with the syn. Consideration of the experimental ionization energies, the transition energies and intensities, compared with theory, leads us to assign the more intense transition at $18\,200\text{ cm}^{-1}$ to the lower energy, anti isomer and the weaker transition, displaced 18 cm^{-1} to higher energy, to the syn isomer.

Table 3 Computational results for various spectroscopic properties for cyclohexadienyl (CD) and several isomers of hydroxy-CHD radical. Results are presented for TD-DFT B3LYP/cc-pvtz level of theory. For the ortho and meta isomers there are two rotamers corresponding to the orientation of the OH bond in syn and anti configurations

Isomer of hydroxy-CHD	Vertical ^a cm ⁻¹	T ₀₀	T ₀₀ (exp)	Calc-exp f (×10 ³)	
syn-ortho	22 097	20 095	18 218 ^e	1877	0.6
anti-ortho	22 327	19 956	18 200 ^e	1756	1.1
syn-meta	21 527	19 867	(17 865) ^f	2003	9.6
anti-meta	20 971	19 531	(17 714) ^f	1817	12
para	19 597	17 225	—	—	14.5
ipso	22 426	— ^d	—	—	1.8
CHD	22 569	20 437	18 207 ^a	2230	0.8

Using the D₁ harmonic vibrational frequencies from these calculations, we have been able to completely assign the spectra of both syn and anti conformers. A complete discussion of this spectroscopic assignment, including the role of in-plane and out-of-plane vibrations, change of OH torsional angle, Fermi resonance and the strengths and weaknesses of the calculations is beyond the scope of this paper. Such detailed spectroscopic analysis does not add to the purpose of this paper, which is a description of ortho-directing nature of the H + phenol reaction. Here, we summarise the key spectroscopic results:

- i. every transition in the REMPI spectrum can be assigned to transitions of the syn and anti conformers of ortho-hydroxy-CHD. No line with any appreciable intensity remains unassigned;
- ii. the assignments can only be made with the anti isomer assigned as the lower frequency, more intense transition, as hypothesized above;
- iii. the most intense transitions for each conformer are loosely associated with the ring-breathing vibration in benzene,⁴⁷ shifted to lower frequency as is common in singly- and di-substituted benzene compounds,^{48,49}
- iv. the calculated minimum energy structure in the D₁ state shows a non-planar distortion of the ring. Assignment of both syn and anti spectra required activity in out-of-plane vibrations. This is consistent with the calculated non-planar structure in the D₁ state;
- v. the syn conformer also shows significant intensity in the vibrational modes loosely affiliated with the ν₆ and ν₁₈ modes in benzene,⁵⁰ again consistent with similar activity in these modes in singly- and di-substituted benzenes.^{48,49}
- vi. calculations show that in-plane and out-of-plane vibrations are significantly more mixed for vibrations of the anti conformer in the D₁ state. There is no analogous vibration for mode 6a in benzene (in-plane ring deformation) for this molecule; the activity is spread through close-lying

levels. This is reflected by several transitions calculated and observed in the vicinity of the 6a vibrational frequency ([Fig. 2](#)). The benzene labels are no longer a good description of the modes in the anti conformer. This effect has been discussed in detail previously for other substituted benzenes.⁵¹

We have indicated a few of the key assignments above the spectrum in [Fig. 2](#). A full description of the spectroscopy of these species, along with the methyl-CHD species, will be published in a forthcoming full spectroscopy paper. Our conclusion for the present work is that the ionization energy, D_1-D_0 frequency, and vibrational frequencies support the REMPI spectrum in [Fig. 2](#) being comprised solely of the syn and anti conformations of the ortho-hydroxy-CHD radical.

Searching for other m/z 95 isomers. We have also performed TD-DFT (B3LYP/cc-pvtz) calculations on the D_1 excited states of the ortho, meta and para isomers of hydroxy-CHD, including syn and anti conformers of the meta isomer. [Table 3](#) shows the calculated vertical transition energies and zero-point energy (zpe) corrected energies, T_{00} , for each isomer. While the vertical calculations for the ipso isomer in the D_1 state did converge, they would not optimize to the minimum of the D_1 state at this level of theory. The calculations appeared to find a conical intersection with the ground electronic state. It is not clear whether this conical intersection is real, or a vagary of the level of theory. Much higher levels of theory will be required to address this. Nonetheless, a vertical transition energy and oscillator strength were able to be calculated and are reported in [Table 3](#).

If we assume that the computational error will be similar (i.e. $2000 \pm 200 \text{ cm}^{-1}$ too high) for the evaluated CHD and ortho-hydroxy-CHD and the, as yet, unobserved isomers, then the meta isomer should absorb in a similar region to that in [Fig. 2](#), while the para isomer is predicted to absorb considerably further to the red, near $15\,000 \text{ cm}^{-1}$. For each radical (including CHD itself), the calculated vertical transition energy is $1900 \pm 500 \text{ cm}^{-1}$ higher than the calculated T_{00} . If we assume the same to be true for the ipso isomer, then we predict this isomer will absorb at about $22\,400 - 1900 - 2000 = 18\,500 \text{ cm}^{-1}$, which also lies within the region shown in [Fig. 2](#).

To search for the other isomers, we performed a series of experiments with the ionization laser wavelength set to 230 nm, while the resonance ($D_1 \leftarrow D_0$) laser was scanned from 617 to 480 nm. This combination of wavelengths provides a total energy of 7.4–8.0 eV, which is in excess of the ionization energy of all isomers according to the calculations in [Table 2](#). The range 617 to 480 nm ($16\,200$ – $20\,800 \text{ cm}^{-1}$) is sufficient to encompass the range of D_1-D_0 energies for all isomers, as shown in [Table 3](#), even allowing for a likely $\sim 9\%$ over-estimate of the theory. The only additional structures found in this range were two small peaks near $17\,714$ and $17\,865 \text{ cm}^{-1}$, as shown in the inset to [Fig. 2](#). The intensity of these peaks is similar, and about $30\times$ weaker than the strong origin bands of ortho-hydroxy-CHD. The peaks were too weak to measure a PIE spectrum. The displacement of the two new peaks from the strong ortho-hydroxy-CHD transitions cannot be assigned readily to low frequency vibrations of ground-state ortho-hydroxy-CHD radical according to our calculations of the vibrational frequencies. Also, their intensity did not seem to scale with that of other hot bands (e.g. just to the red of the origin transitions). Therefore they do not seem to be hot bands of the ortho-hydroxy-CHD spectrum.

The two new transitions are about 500 cm^{-1} lower than the ortho-hydroxy-CHD origin and this difference is in accord with that calculated for the meta hydroxy-CHD radical relative to the ortho isomer. In addition, their larger splitting of 150 cm^{-1} is in accord with the larger calculated syn–anti splitting, and the similar intensity is consistent with the calculated oscillator strengths (Table 3). Therefore we tentatively assign these two peaks to the syn and anti rotamers of the meta species. If this assignment is correct, then the meta isomer is formed at <1% of the population of the ortho, given the 30× weaker spectrum, and 10× higher oscillator strength. However, we cannot conclusively rule out hot bands, nor a different constitutional isomer of $\text{C}_6\text{H}_7\text{O}$ and this assignment must be considered to be tentative.

The ipso isomer has a calculated $D_1 \leftarrow D_0$ transition energy that is similar to that of the ortho (Table 3). Hole burning shows that all major peaks in Fig. 2 are attributable to the ortho isomers. However, the lower signal-to-noise ratio of the hole-burning spectra makes it difficult to conclude that the spectrum of the ipso isomer is not hiding in the weaker, more complex structure at the blue end of this spectrum. Therefore we used the fact that the calculated IEs for ortho and ipso isomers are quite different and re-measured the REMPI spectrum of Fig. 2 using an ionization energy of 6.7 eV, which is significantly below that of ipso according to our calculations. The ensuing spectrum did not reveal any missing peaks, compared with the spectrum in Fig. 2. Therefore we have found no evidence of any spectral signature of the ipso isomer in the spectral range 480–617 nm.

We conclude that, in a molecular beam resulting from discharge of phenol/water/argon, the resulting H-atom reaction with phenol produces predominantly the ortho-hydroxy-CHD radical. There is no evidence for para or ipso, and there is tentative evidence for <1% meta isomer.

H and D-addition to toluene: methylcyclohexadienyl radical (methyl-CHD)

A similar set of experiments was performed for the reaction of H-atoms with toluene. Fig. 5 shows the $(1 + 1')$ REMPI spectrum of a molecule(s) with m/z 93, the mass of H + toluene. The PIE curve, measured when the first REMPI laser was tuned to the large peak near $18\,250\text{ cm}^{-1}$, is shown at the top of Fig. 3. After correction for the extraction field in the same way as previously, the IE of this molecule was determined to be $6.5862(5)\text{ eV}$.¹³

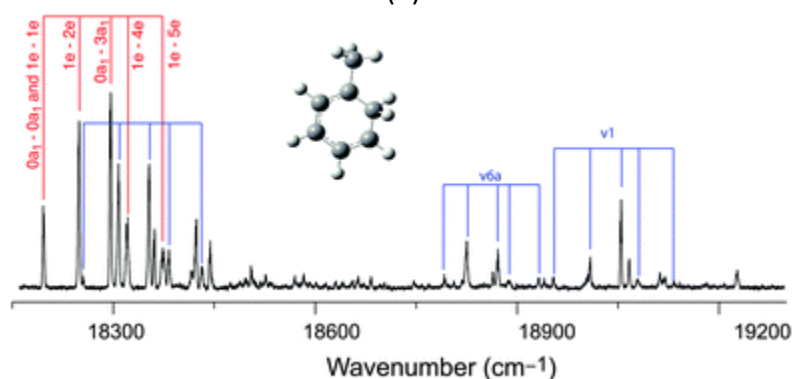


Fig. 5 REMPI spectrum of the m/z 93 species formed from H-addition to toluene. The carrier of the spectrum is assigned to be ortho-methyl-cyclohexadienyl radical. The origin torsional progression is assigned, and three other torsional progressions are identified (see text).

The same set of calculations, at the same level of theory, was performed on the four isomers of methyl-CHD ([Table 4](#)). At this level of theory, we empirically correct the IEs by -80 meV, in keeping with the benchmark study above, and also validated by the results on the hydroxy-CHD radical. The corrected IE of the ipso isomer clearly does not match the experimental value. The IEs of the ortho, meta and para isomers are clustered more closely together than they were for hydroxy-CHD. Nonetheless, attribution of the m/z 93 carrier of the peak at $18\,250\text{ cm}^{-1}$ to the ortho isomer is the only one that lies within the computational uncertainty, which we estimate at <100 meV.⁵²

Table 4 Computational results for various properties of the four isomers of methyl-cyclohexadienyl radical (methyl-CHD). Results are presented for the G4(MP2)-6X level of theory; results for other levels of theory are reported in ESI. All values in kJ mol^{-1} , except for the IE, in eV

Property	ips			
	ortho	meta	para	o
Geometries optimized at B3-LYP/6-31G(2df,p).				
Relative energy of methyl-CHD	0.0	5.4	6.5	10.5
Relative energy of methyl-CHD cation	5.9	19.7	0.0	33.7
C–H bond dissociation energy, vibrationless	115	110	109	105
C–H BDE, zpe corrected, 0 K	93	88	87	81
Ionization energy, vibrationless (eV)	6.63	6.72	6.50	6.81
Ionization energy, zpe corrected, 0 K (eV)	6.67	6.76	6.54	6.85
Ionization energy, empirically corrected, 0 K (eV)	6.59	6.68	6.46	6.77
Ionization energy, corrected experimental (eV)	6.5862 ± 0.0005			

The REMPI spectrum in [Fig. 5](#) shows a complex set of close, but irregularly spaced peaks in the region assigned as the electronic origin. By analogy with the spectroscopy of toluene^{53–58} and singly-substituted toluenes,^{59–61} this structure is assigned as arising from methyl-rotor torsional vibrations. Methyl-rotor structure in toluene itself and in substituted toluenes, has been well studied. The methyl-rotor torsional states are of very low energy, and the spacing between levels depends sensitively on the height and form of the torsional barrier. In toluene, and toluene with other atoms substituted in the para-position, the potential is six-fold symmetric. Introduction of a substituent at the ortho or meta position introduces a three-fold term into the potential.

The energy levels of the internal rotation of the methyl rotor are usually represented by the quantum number of a free one-dimensional rotor, m , where $m = 0, \pm 1, \pm 2, \dots$. For a free rotor, the levels have energy proportional to m^2 . For a hindered rotor, the energy level spacings are irregular, with the energies a sensitive function of the shape of the torsional potential. For a potential with three-fold symmetry, such as ortho-methyl-CHD, the levels have symmetry designations of a and e. The $m = \pm 3n$ levels (where n is an integer) are of a symmetry, while $m = 3n \pm 1$ levels are e.

Electronic transitions between different methyl rotor states are subject to symmetry selection rules. For a potential with six-fold symmetry, the transitions are dominated by $\Delta m = 0$, although $\Delta m = 3$ are

also observed. The recent papers by Lawrance and co-workers provide an excellent description of methyl-rotors in the spectroscopy of toluene.⁵⁶ For a potential of three-fold symmetry, the selection rules are $a \leftrightarrow a$ and $e \leftrightarrow e$.

The methyl-rotor vibrational structure in the electronic spectrum is also a sensitive function of the change in torsional potential upon electronic excitation. In toluene and p-fluorotoluene, there is little change in the equilibrium rotor position and the spectrum shows only weak activity in the methyl rotor modes.⁵⁹ In ortho-substituted toluene, the V_3 term is much larger than in the meta-substituted counterparts, due to the increased steric interaction.⁵⁹ The change in V_3 can also be significant upon electronic excitation for the ortho-species; in fluorotoluene, the minimum in S_0 becomes a maximum in S_1 .⁵⁹ For the meta equivalent, the minimum lies at the same angle in S_0 and S_0 , with the consequence that the torsional structure in m-fluorobenzene is also dominated by $\Delta m = 0$.⁵⁹ The extensive torsional structure in the spectrum in [Fig. 5](#) is therefore consistent with the formation of ortho-methyl-CHD, and not meta or para.

There are more peaks in the origin region than can be accounted for by a single methyl rotor progression and it is clear that other low frequency vibrations play an important part of the spectroscopy in this region. Other vibrations, however, can have a profound effect on the torsional potential.^{57,58} For example, the ring-breathing vibration, ν_1 , and in-plane ring-distortion, ν_6 , again form the dominant progressions in [Fig. 5](#). Each has a similar set of torsional transitions associated with them. The spacings between the peaks in the ν_1 progression are similar, but not exactly the same, as the origin region. For the ν_6 progression, however, they are quite different, which is apparent by eye in [Fig. 5](#).

To untangle the spectrum, we have performed the same experiment using a combination of deuterated toluenes (toluene- d_3 , and - d_8) and normal and deuterated water (D_2O). This gives rise to 6 different isotopologues of ortho-methyl-CHD. The torsional energy levels shift significantly when the CH_3 -group is deuterated, as expected, but not so much when the CH_2 group is deuterated. This has allowed us to unpack the spectrum and separate low frequency skeletal vibrations from methyl torsion vibrations. The torsional structure for the origin is assigned in [Fig. 5](#), along with the torsional structure neighboring the ν_{6a} and ν_1 progressions. Another torsional progression is indicated threaded through the origin series, which has its origin in one of the low frequency out-of-plane skeletal vibrations.

The experiments on specifically deuterated toluene and water were also used to clarify another aspect of the H + toluene reaction, which is important in later discussion of the H-addition mechanism. The resultant m/z 94 (D + toluene) REMPI spectrum is almost identical to that for the fully hydrogenated radical, evincing a CH_3 rotor (i.e. no D-atom substitution on the rotor position). No evidence of other isotopomers (D-addition elsewhere on the ring or on the rotor) was found. In addition, no evidence for other isotopologues (greater substitution of D-atoms) was found in the mass spectrum.

Experiments were further repeated using toluene- d_3 (CD_3 rotor) and toluene- d_8 reacting with both H atoms and D atoms. In every case, we only observed single addition of H/D to the ortho site on the ring – no other isomers, and no additional substitution of H for D, or vice versa.

The above observations indicate clearly that the H-addition process for toluene (and presumably phenol) is a single-step kinetic pathway. The spectra show clearly that there is no intramolecular H/D exchange. The mass spectra show clearly that there are no sequential reactions involving H/D-addition, followed by H/D loss that would otherwise scramble the resultant isotopologues, resulting in new mass channels. These observations provide strong evidence that the observed radicals are the result of a single H or D-addition reaction. If the ortho-methyl-CHD(-d₁) radical that is formed from the toluene + D reaction spontaneously lost H or D from the sp³ site, then both toluene-d₀ and toluene-d₁ would be formed. Subsequent reaction of D atoms with toluene-d₁ would lead to two isomers of ortho-methyl-CHD(-d₂), with either both D atoms on the same carbon, or with D substitution on both ortho positions. Sequential addition/loss reactions would lead to increasing deuteration of the radical at the ortho position, an effect that was not observed.

Again, we searched for evidence of the para, meta and ipso isomers by scanning up to 2000 cm⁻¹ to higher and lower frequency than the ortho origin bands. Spectra were re-taken with different ionization energies and no features in the spectrum appeared or disappeared. Therefore, like hydroxy-CHD, we conclude that only the ortho-methyl-CHD radical is formed to a significant extent in these experiments.

A complete analysis of the spectrum in [Fig. 5](#) and spectra of the isotopologues of methyl-CHD, including fitting the torsional potential in both D₀ and D₁ states of all 6 isotopologues, is beyond the scope of the present work. This extensive spectroscopic work will be published in a forthcoming paper.

Discussion

The results above report the D₁ ← D₀ spectra of ortho-methyl-cyclohexadienyl radical and both syn and anti conformers of the ortho-hydroxy-CHD radical, which were formed from H-addition to toluene and phenol, respectively. The spectra have sharp structure in each case, with well-resolved vibrational transitions, and a D₁ lifetime for hydroxy-CHD that has been measured in the 3–5 ns range. Adiabatic (0 K) ionization energies were measured for each isomer.

Ab initio and DFT calculations support the experimental results. Benchmarking to the CHD radical provided an empirical correction for the ionization energies calculated using G4(MP2)-6X theory. When this correction was applied to calculations on the ortho-methyl- and ortho-hydroxy-CHD radicals, the experimental IEs were reproduced to within 10 meV.

The most intriguing aspect of this work is that we have identified and assigned only the ortho isomer for H-atom addition to phenol and toluene. No evidence was found for the formation of the ipso or para isomers. Tentative evidence for a small amount of the meta isomer of hydroxy-CHD was presented, but no evidence of the meta isomer for the methyl-substituted radical. It is this aspect of the H-addition chemistry that we focus on in this discussion.

Ab initio calculations on H-addition to phenol and toluene

[Fig. 6](#) shows the energies for stationary points on the reaction paths for H-addition to phenol and toluene, OH- or CH₃-addition to benzene, and [1,2]-H shifts between the various substituted

cyclohexadienyl radical isomers. The calculations were performed at a single level of theory, vis G4(MP2)-6X//B3-LYP/6-31G(2df,p). In both cases, the ortho isomer is the most stable, lying 12–13 kJ mol⁻¹ below meta and para for the hydroxy-CHD radical, but only 5–7 kJ mol⁻¹ lower for methyl-CHD. The ipso isomer, which is the essential isomer connecting H + phenol (toluene) and OH (CH₃) + benzene, lies 32 and 11 kJ mol⁻¹ higher in the respective radicals. Not shown in the figure are the syn and anti conformers of the meta and ortho isomers.

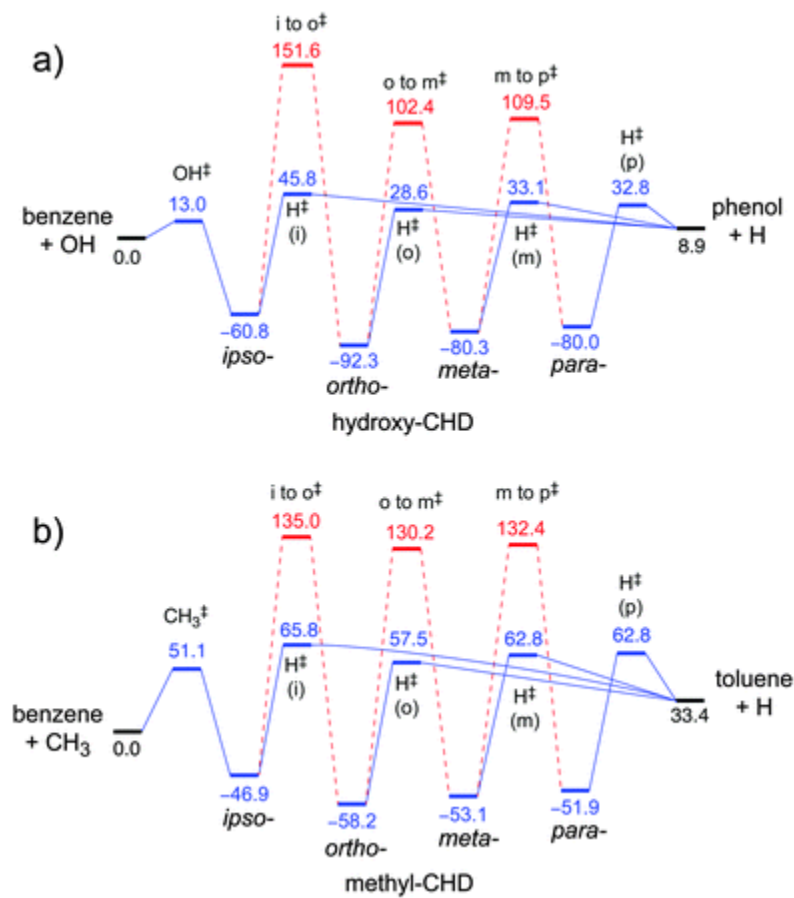


Fig. 6 Energies (kJ mol⁻¹, 298 K) for stationary points on the reaction paths for (a) H-addition to phenol through OH-addition to benzene and 1,2-H-transfer between the isomers of hydroxy-cyclohexadienyl radical; (b) H-addition to toluene through CH₃-addition to benzene and 1,2-H-transfer between isomers of methyl-cyclohexadienyl radical. [‡ represents a transition structure.] Values are calculated at G4(MP2)-6X//B3-LYP/6-31G(2df,p).

The hydroxy-CHD potential energy surface. Some of these energies and pathways have been calculated previously for hydroxy-CHD,^{27–29} but, to our knowledge, none of the previous studies characterized all of the isomers and transition structures. Consequently, there is not a complete picture of the chemistry from benzene + OH to phenol + H that includes all the isomers and transition states such as shown in [Fig. 6a](#).

The most studied part of this potential energy surface is the benzene + OH reaction because of its importance in atmospheric and combustion chemistry. This reaction leads solely to the ipso isomer, although other reaction products, including displacement of OH for H leading directly to phenol, have also been postulated to be competitive with OH-addition.^{26,30} Previous calculations of the stability of

the ipso isomer lie in the range -66 to -78 kJ mol^{-1} relative to phenol + H with an entrance channel barrier of 26 to 41 kJ mol^{-1} .²⁷⁻²⁹ The energies of the other isomers have been calculated by Sander et al.²⁷ Their hydroxy-CHD energies are slightly lower with respect to phenol + H than ours, but were not corrected for zpe. Our uncorrected energies ([Table 2](#)) are similar to the previous values.

Given the observation of only the ortho isomer, which is most stable, we were interested in whether (1,2)-H transfer between isomers might be possible. The TS energies for transfer from ipso-ortho, ortho-meta and meta-para were therefore calculated. The results displayed in [Fig. 6](#) show clearly that the TSs lie significantly (>100 kJ mol^{-1}) above the TS for breaking the C-H bond. The same phenomenon has been calculated for H-D scrambling in CHD radical itself – the energy of the TS for [1,2]-H shift in CHD was twice as high as that for removing the sp^3 H-atom.^{32,62}

The potential energy surface for the methyl-CHD radical is quite similar to that of the OH analog ([Fig. 6b](#)). [1,2]-H shifts in methyl-CHD have transition states that lie well above the TS for C-H cleavage, which is ~ 110 kJ mol^{-1} . The energy ordering of the isomers is the same: ortho < meta < para < ipso. But ortho is favoured by only 5–7 kJ mol^{-1} . The entrance channel barriers from toluene + H into the methyl-CHD wells are larger than for phenol + H, being ~ 30 kJ mol^{-1} instead of ~ 20 kJ mol^{-1} . The ortho TS remains the lowest, with a difference between this and the para and meta TSs still ~ 5 kJ mol^{-1} .

Therefore we conclude that the observed preference for ortho-addition of H to toluene and phenol must lie in the formation process, rather than subsequent migration of the H-atom around the ring.

Is the detection method biased towards ortho?

Our characterization technique is (1 + 1') resonance-enhanced multiphoton ionization coupled with time-of-flight mass spectrometry. The energy of D_1 is clearly well above the C-H bond dissociation energy and hence the transition is pre-dissociative. Therefore we must consider the possibility that the ortho isomer is longer-lived in the D_1 state than the other isomers. The measured lifetime of the ortho isomer is 3–5 ns. However, we have been successful in detecting radicals with excited state lifetimes as short as ~ 100 ps, inferred from their spectral linewidth. Therefore the lifetime of the other hydroxy- or methyl-CHD isomers would therefore need to be $>50\times$ shorter than that of the observed ortho isomers for REMPI to be an ineffective technique. Given the very similar electronic properties of the four isomers, we have no reason to suspect that this is so.

We also note a much older work by Bennett and Mile in 1973.⁶³ In this remarkable, but little cited work, they measured the products of H and D addition to ~ 30 unsaturated and aromatic compounds by bombardment of a cold matrix of olefin by H/D atoms. They observed that for toluene [$\varphi\text{-CH}_3$], benzyl alcohol [$\varphi\text{-CH}_2\text{OH}$] and cumene [$\varphi\text{-CH}(\text{CH}_3)_2$], the H/D addition occurs solely at the ortho position. In contrast to our work, they observed a much smaller amount of para isomer, and no evidence of meta. The notable feature for the present discussion is that their detection technique was ESR spectroscopy, which has no bias towards ortho, meta or para and no reliance on excited state spectroscopy. Therefore we conclude that the addition of H to toluene and phenol is ortho-directed.

Energetic considerations

The ortho isomer is the lowest lying of the isomers, for both hydroxy- and methyl-CHD. It lies 12–13 kJ mol⁻¹ below meta and para for the OH structure, but only 5–7 kJ mol⁻¹ lower for the CH₃ structure. Our first consideration, therefore, is whether energetic considerations alone can account for the ortho preference.

Generally, a supersonic expansion of discharge products is not a discriminating technique. Many radicals are formed – not solely the thermodynamically-favoured product. For example, in the same instrument we observed the cis and trans-vinylpropargyl molecule (C₅H₅),⁶⁴ even though it lies 130 kJ mol⁻¹ above the global minimum, the c-pentadienyl radical.⁶⁵ Even in the present work, both syn and anti conformers of ortho-hydroxy-CHD are observed strongly even though syn lies 6 kJ mol⁻¹ above the anti. This is similar to the energy difference between ortho and para/meta-methyl-CHD (5–7 kJ mol⁻¹), yet only ortho is observed. Therefore it seems unlikely that the preference for the ortho-isomers is driven by thermodynamics alone.

Kinetic considerations

The height of the barrier in the entrance channel determines the kinetic preference for various isomers. For both substituted-CHD radicals, the ortho isomer has the lowest energy entrance channel barrier of the four structural isomers. For OH, this is 20 kJ mol⁻¹, compared with 24 kJ mol⁻¹ for both meta and para, and 37 kJ mol⁻¹ for the ipso isomer. For CH₃, the entrance barriers are: 24 kJ mol⁻¹ for ortho, 29 kJ mol⁻¹ for para and meta and 32 kJ mol⁻¹ for ipso.

The collision conditions in a discharge expansion are difficult to characterize. Collisions within the region of the electrodes can be very energetic, but collisions late in the supersonic expansion are considerably colder than room temperature. If we assume that the entrance channels are similar in topology (entropy), then, working in reverse, we can calculate the effective temperature required to achieve an order of magnitude difference in formation rate, given the barriers in [Fig. 6](#). For a difference in barrier height of 4 kJ mol⁻¹ in the entrance channel (hydroxy-CHD), a collision temperature of 200 K would produce a ten-fold enhancement in reaction rate for the compound with the lower barrier compared with the higher barrier channel, irrespective of the barrier height (exclusive of symmetry effects, which enhances ortho and meta over para and ipso by a further factor of two based upon the number of identical sites). At 100 K, the difference would be 100-fold. Indeed, a translational temperature of 100–200 K is what would be expected in the early stages of a supersonic expansion.

At this stage, it is appropriate to consider the experiments on deuterium addition to toluene. As discussed above, when D₂O was used instead of H₂O, the only product was methyl-CHD-d₁. If the reaction proceeded at high translational temperature, one would expect that some of the transiently formed methyl-CHD radicals would spontaneously decompose back to toluene + H/D. Consideration of zero-point energy for H-loss and D-loss would favour the H-loss channel, so we would expect methyl-CHD-d₁ to produce a significant amount of toluene-d₁ + H, which would then further react with D atoms to form methyl-CHD-d₂. We observed no evidence of the -d₂ isotopologue in the mass spectrum. Therefore we conclude that there is no further processing of toluene via reaction with D-atoms. This is best explained by requiring the energy of the first D + toluene reaction to be fairly low, so that a single

collision with the cold Ar carrier gas stabilizes the methyl-CHD radical. This is consistent with a collision temperature of 100–200 K.

Finally, it is pertinent to consider the effect of tunneling of H-atoms in both the formation and decomposition of substituted CHD radicals. The principal effect of tunneling is to lower the effective barrier for both H-addition and H-loss channels. If the effects of tunneling are similar for all isomers, then this has no effect on the discussion above; the preference for one channel over another depends on the difference in barrier height, not the barrier height itself. Lowering the barrier of both channels by the same amount will increase the rate of reaction (increasing the signal in the experiment), but it will not change the relative yield of one channel over another.

We therefore conclude that our data are consistent with a preference for ortho-addition to phenol and toluene caused by a kinetic effect at a temperature of 100–200 K.

Implications for combustion modeling

Rate constants for the reactions of H-atoms with benzene, phenol and toluene have all been measured for a wide range of temperatures relevant to combustion.⁶⁶ The competition between H-abstraction and H-addition is a sensitive function of temperature. As a general rule, the importance of abstraction over addition increases with temperature. For example, at $T < 600$ K, the rate constant for H-addition to toluene to form methyl-CHD, is larger than H-abstraction to form H_2 + benzyl radical, or benzene + CH_3 . For $T > 600$ K, both abstraction reactions have rate constants that are larger than the H-addition.⁶⁶ Similarly, for H + benzene, H-addition is the only important mechanism for all except the most elevated combustion temperatures.⁶⁶

Despite the importance of H-addition to aromatic species in combustion, there are no studies in which the isomer-specific products of such addition have been elucidated. In this work, we determined that H-addition to phenol and toluene, at a temperature of 100–200 K is significantly (>10-fold) ortho-directed. When taken in concert with the results of Bennett and Mile,⁶³ it is strongly suggestive that preferential ortho-addition is the norm for many singly-substituted benzenes.

Using the energetics (barriers) and relative kinetics employed above, we can predict the ortho-directing effect at increased temperatures more relevant to combustion. Using the calculated barriers for toluene in Fig. 6b, we predict that at 600 K, ortho-methyl-CHD would be kinetically-preferred over meta by a factor of ~ 3 , and over para by ~ 6 , due to symmetry considerations. ipso remains less favoured by more than a factor of 10 for methyl-CHD at this temperature.

At 2000 K, the predicted relative rates still favour the formation of the ortho product, with a ratio of ortho : meta : para : ipso of 1 : 0.7 : 0.35 : 0.3. At even more elevated temperatures, the relative rates of formation of ortho, meta, para and ipso converge on the symmetry-imposed ratio of 1 : 1 : 0.5 : 0.5.

Conclusions

We have studied the formation of hydroxy- and methyl-cyclohexadienyl radicals via the reaction of H and D atoms with phenol and toluene, respectively. The 1 + 1' REMPI spectrum and the adiabatic

ionization energies of these species are reported. The experiments were accompanied by extensive quantum chemical calculations, which were benchmarked to the well-known cyclohexadienyl radical. We report calculated energies and structures for ortho, meta, para and ipso isomers of the two substituted-CHD radicals, including syn and anti conformers of ortho and meta isomers. Transition structures for H migration around the ring are reported, as are the transition structures for both H + toluene/phenol and OH/CH₃ + benzene.

In all cases, the REMPI spectra can be assigned solely to H-atom attachment at the ortho position. There is no experimental evidence for any other isomer, except for a hint of meta-hydroxy-CHD in the H + phenol experiments. For the case of D-addition, no further deuteration other than a single D-atom was observed, attesting to H/D addition being a primary reaction with no recycling of H and D atoms via the reverse reaction.

We attribute the greater than tenfold preference for formation of ortho radicals to the height of the barrier in the entrance channel to the reaction, which is 4–5 kJ mol⁻¹ lower for ortho than meta and para and even further below the ipso channel. Under the conditions of these experiments, this is consistent with formation of the radicals at a collision temperature of 100–200 K, appropriate for the early stages of a molecular beam expansion. Under pre-ignition conditions in combustion (T = 200–400 °C), we predict ortho to be still the significantly preferred product. Only at an elevated temperature (T > 2000 °C) would the formation rate of the three lower-energy isomers approach the statistical ratio of 1 : 1 : 0.5 : 0.5 for ortho : meta : para : ipso.

Acknowledgements

This work was supported by the Australian Research Council (grant DP120102559). CMW acknowledges an Australian Postgraduate Award scholarship. We gratefully acknowledge generous allocations of supercomputer time from the National Computational Infrastructure (NCI) National Facility and Intersect Australia Ltd.

References

- ¹For example, C. K. Westbrook, *Combust. Flame*, 2009, 156, 181 .
- ²For example, B. J. Finlayson-Pitts and J. N. Pitts Jr., *Chemistry of the Upper and Lower Atmosphere*, Academic Press, 2000 .
- ³D. U. Andrews, B. R. Heazlewood, A. T. Maccarone, T. Conroy, R. J. Payne, M. J. T. Jordan and S. H. Kable, *Science*, 2012, 337, 1203 .
- ⁴For example, J. A. Rasmussen, *J. Phys. Chem. A*, 2013, 117, 4279.
- ⁵E. Habart, F. Boulanger, L. Verstraete, G. Pineau des Forets, E. Falgarone and A. Abergel, *Astron. Astrophys.*, 2003, 397, 623
- ⁶D. L. Kokkin and T. W. Schmidt, *J. Phys. Chem. A*, 2006, 110, 6173 .
- ⁷Fuel Standard (Petrol) Determination 2001, ComLawId: F2008C00344, Office of Legislative Drafting and Publishing, Commonwealth of Australia.
- ⁸A. Tesner, *Proc. Combust. Inst.*, 1958, 7, 546.
- ⁹T. Bera, J. W. Thybaut and G. B. Marin, *Ind. Eng. Chem. Res.*, 2011, 50, 12933.
- ¹⁰T. Shida and I. Hanazaki, *Bull. Chem. Soc. Jpn.*, 1970, 43, 646.
- ¹¹T. Imamura, W. Zhang, H. Horiuchi, H. Hiratsuka, T. Kudo and K. Obi, *J. Chem. Phys.*, 2004, 121, 6861.
- ¹²M. Nakajima, T. W. Schmidt, Y. Sumiyoshi and Y. Endo, *Chem. Phys. Lett.*, 2007, 449, 57.

- ¹³O. Krechkivska, C. Wilcox, G. D. O'Connor, K. Nauta, S. H. Kable and T. W. Schmidt, *J. Phys. Chem. A*, 2014, 118, 10252.
- ¹⁴A. Bonaca and G. Bilalbegović, *Mon. Not. R. Astron. Soc.*, 2011, 416, 1509–1513.
- ¹⁵J. A. Sebree, V. V. Kislov, A. M. Mebel and T. S. Zwier, *J. Phys. Chem. A*, 2010, 114, 6255–6262.
- ¹⁶M. Bahou, Y.-J. Wu and Y.-P. Lee, *Phys. Chem. Chem. Phys.*, 2013, 15, 1907–1917.
- ¹⁷O. Krechkivska, Y. Liu, K. L. K. Lee, K. Nauta, S. H. Kable and T. W. Schmidt, *J. Phys. Chem. Lett.*, 2013, 4, 3728.
- ¹⁸O. Krechkivska, C. M. Wilcox, B. Chan, R. Jacob, Y. Liu, K. Nauta, S. H. Kable, L. Radom and T. W. Schmidt, *J. Phys. Chem. A*, 2015, 119, 3225.
- ¹⁹J. G. Calvert, R. Atkinson, K. H. Becker, R. M. Kamens, J. H. Seinfeld, T. J. Wallington and G. Yarwood, *The Mechanisms of Atmospheric Oxidation of Aromatic Hydrocarbons*, Oxford University Press, New York, 2002.
- ²⁰A. Bargholz, R. Oswald and P. Botschwina, *J. Chem. Phys.*, 2013, 138, 014307.
- ²¹W. H. Hamill, J. P. Guarino, M. R. Ronayne and J. A. Ward, *Discuss. Faraday Soc.*, 1963, 36, 169.
- ²²J. E. Jordan, D. W. Pratt and D. E. Wood, *J. Am. Chem. Soc.*, 1974, 96, 5588.
- ²³I. Garkusha, J. Fulara, A. Nagy and J. P. Maier, *J. Am. Chem. Soc.*, 2010, 132, 14979.
- ²⁴C.-C. Chen, J. W. Bozzelli and J. T. Farrell, *J. Phys. Chem. A*, 2004, 108, 4632.
- ²⁵R. Volkamer, B. Klotz, I. Barnes, T. Imamura, K. Wirtz, N. Washida, K. H. Becker and U. Platt, *Phys. Chem. Chem. Phys.*, 2002, 4, 1598.
- ²⁶B. Fritz, V. Handwerk, M. Preidel and R. Zellner, *Ber. Bunsen-Ges.*, 1985, 89, 343.
- ²⁷A. Mardyukov, R. Crespo-Otero, E. Sanchez-Garcia and W. Sander, *Chem. – Eur. J.*, 2010, 16, 8679.
- ²⁸C.-C. Chen, J. W. Bozzelli and J. T. Farrell, *J. Phys. Chem. A*, 2004, 108, 4632.
- ²⁹I. V. Tokmakov and M. C. Lin, *J. Chem. Phys.*, 2002, 116, 11309.
- ³⁰E. Bjergbakke, A. Sillesen and P. Pagsberg, *J. Phys. Chem.*, 1996, 100, 5729.
- ³¹V. H. Uc, A. Hernandez-Laguna, A. Grand and A. Vivier-Bunge, *Phys. Chem. Chem. Phys.*, 2002, 4, 5730.
- ³²I. V. Tokmakov and M. C. Lin, *Int. J. Chem. Kinet.*, 2001, 33, 633.
- ³³N. J. Reilly, M. Nakajima, T. P. Troy, N. Chalyavi, K. A. Duncan, K. Nauta, S. H. Kable and T. W. Schmidt, *J. Am. Chem. Soc.*, 2009, 131, 13423.
- ³⁴H. Snyder, B. Smith, T. Parr and R. Martin, *Chem. Phys.*, 1982, 65, 397.
- ³⁵M. J. Frisch, G. W. Trucks, H. B. Schlegel, G. E. Scuseria, M. A. Robb, J. R. Cheeseman, G. Scalmani, V. Barone, B. Mennucci and G. A. Petersson, et al., *Gaussian 09, Revision A.02*, Gaussian, Inc., Wallingford, CT, 2009.
- ³⁶H.-J. Werner, P. J. Knowles, G. Knizia, F. R. Manby, M. Schütz, P. Celani, T. Korona, R. Lindh, A. Mitrushenkov and G. Rauhut, et al., *MOLPRO, 2010.1*, University College Cardiff Consultants Limited, Cardiff, UK, 2010.
- ³⁷D. J. Henry, M. J. Sullivan and L. Radom, *J. Chem. Phys.*, 2003, 118, 4849–4860.
- ³⁸B. Chan, J. Deng and L. Radom, *J. Chem. Theory Comput.*, 2011, 7, 112–120.
- ³⁹B. Chan and L. Radom, *J. Chem. Theory Comput.*, 2012, 8, 4259–4269.
- ⁴⁰A. D. Boese and J. M. L. Martin, *J. Chem. Phys.*, 2004, 121, 3405–3416.
- ⁴¹J. P. Merrick, D. Moran and L. Radom, *J. Phys. Chem. A*, 2007, 111, 11683–11700.
- ⁴²A. J. Birch, A. L. Hinde and L. Radom, *J. Am. Chem. Soc.*, 1980, 102, 4075.
- ⁴³F. Berho, M.-T. Rayez and R. Lesclaux, *J. Phys. Chem. A*, 1999, 103, 5501.
- ⁴⁴Gas Phase Ion Energetics Data, in *NIST Chemistry WebBook*, NIST Standard Reference Database Number 69, ed. P. J. Linstrom and W. G. Mallard, National Institute of Standards and Technology, Gaithersburg MD, 2016, <http://webbook.nist.gov>, accessed 3-March-2016.
- ⁴⁵D. Aue, M. Guidoni and L. Betowski, *Int. J. Mass Spectrom.*, 2000, 201, 283.
- ⁴⁶E. P. L. Hunter and S. G. Lias, *J. Phys. Chem. Ref. Data*, 1998, 27, 413.
- ⁴⁷E. B. Wilson Jr., *Phys. Rev.*, 1934, 45, 706.
- ⁴⁸P. Butler, D. B. Moss, H. Yin, T. W. Schmidt and S. H. Kable, *J. Chem. Phys.*, 2007, 127, 094303.
- ⁴⁹A. K. Swinn and S. H. Kable, *J. Mol. Spectrosc.*, 1998, 191, 49.
- ⁵⁰G. H. Atkinson and C. S. Parmenter, *J. Mol. Spectrosc.*, 1978, 73, 52.

- ⁵¹A. G. Gardner and T. G. Wright, *J. Chem. Phys.*, 2011, 135, 114305.
- ⁵²T. P. Troy, N. Chalyavi, A. S. Menon, G. D. O'Connor, B. Fückel, K. Nauta, L. Radom and T. W. Schmidt, *Chem. Sci.*, 2011, 2, 1755.
- ⁵³P. J. Breen, J. A. Warren, E. R. Bernstein and J. I. Seeman, *J. Chem. Phys.*, 1987, 87, 1917.
- ⁵⁴D. B. Moss, C. S. Parmenter and G. E. Ewing, *J. Chem. Phys.*, 1987, 86, 51.
- ⁵⁵A. M. Gardner, A. M. Green, V. M. Tamé-Reyes, V. H. K. Wilton and T. G. Wright, *J. Chem. Phys.*, 2013, 138, 134303.
- ⁵⁶J. R. Gascooke and W. D. Lawrance, *J. Chem. Phys.*, 2013, 138, 134302.
- ⁵⁷J. R. Gascooke, E. A. Virgo and W. D. Lawrance, *J. Chem. Phys.*, 2015, 142, 024315.
- ⁵⁸J. R. Gascooke, E. A. Virgo and W. D. Lawrance, *J. Chem. Phys.*, 2015, 143, 044313.
- ⁵⁹K. Okuyama, N. Mikami and M. Ito, *J. Phys. Chem.*, 1985, 89, 5617.
- ⁶⁰Z.-Q. Zhao, C. S. Parmenter, D. B. Moss, A. J. Bradley, A. E. W. Knight and K. G. Owens, *J. Chem. Phys.*, 1992, 96, 6362.
- ⁶¹T.-Y. D. Lin and T. A. Miller, *J. Phys. Chem.*, 1990, 94, 3554.
- ⁶²O. Kikuchi and S. Shimomura, *Bull. Chem. Soc. Jpn.*, 1984, 57, 2993.
- ⁶³J. E. Bennett and B. Mile, *J. Chem. Soc., Faraday Trans.*, 1973, 69, 1398.
- ⁶⁴N. J. Reilly, M. Nakajima, T. P. Troy, N. Chalyavi, K. A. Duncan, K. Nauta, S. H. Kable and T. W. Schmidt, *J. Am. Chem. Soc.*, 2009, 131, 13423.
- ⁶⁵L. V. Moskaleva and M. C. Lin, *J. Comput. Chem.*, 1999, 21, 415.
- ⁶⁶D. L. Baulch, et al. , *J. Phys. Chem. Ref. Data*, 2005, 34, 757.